Visualizing Symmetric Indefinite 2D Tensor Fields Using the Heat Kernel Signature

Valentin Zobel, Jan Reininghaus, and Ingrid Hotz

Abstract The Heat Kernel Signature (HKS) is a scalar quantity which is derived from the heat kernel of a given shape. Due to its robustness, isometry invariance, and multiscale nature, it has been successfully applied in many geometric applications. From a more general point of view, the HKS can be considered as a descriptor of the metric of a Riemannian manifold. Given a symmetric positive definite tensor field we may interpret it as the metric of some Riemannian manifold and thereby apply the HKS to visualize and analyze the given tensor data. In this paper, we propose a generalization of this approach that enables the treatment of indefinite tensor fields, like the stress tensor, by interpreting them as a generator of a positive definite tensor field. To investigate the usefulness of this approach we consider the stress tensor from the two-point-load model example and from a mechanical work piece.

1 Introduction

The Heat Kernel Signature (HKS) is a powerful shape signature and has been introduced by Sun et al. in [11]. They have shown that the HKS is an isometric invariant and contains almost all intrinsic information of a surface. Intuitively, the HKS can be considered as the curvature of the surface. Since the HKS is derived from the process of heat diffusion it is equipped with a time parameter which is a measure for the size of the neighborhood that influences the value of the HKS at a point. Common applications use the HKS to detect similarly shaped surfaces, see [2, 4, 7, 8].

V. Zobel (✉)
Leipzig University, Leipzig, Germany
e-mail: zobel@informatik.uni-leipzig.de

J. Reininghaus
Institute of Science and Technology Austria, Klosterneuburg, Austria
e-mail: jan.reininghaus@ist.ac.at

I. Hotz
Linköping University, Norrköping, Sweden
e-mail: ingrid.hotz@liu.se

I. Hotz, T. Schultz (eds.), *Visualization and Processing of Higher Order Descriptors for Multi-Valued Data*, Mathematics and Visualization,
DOI 10.1007/978-3-319-15090-1_13

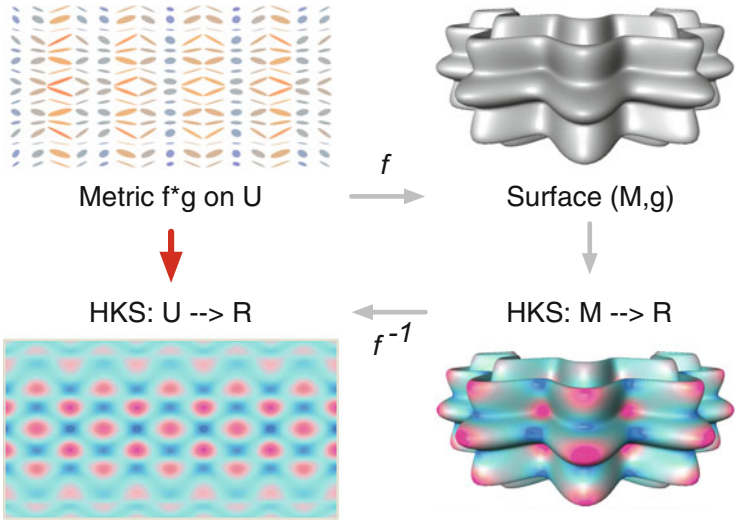

Fig. 1 Commutative diagram illustrating the relation between the HKS of a surface and a positive definite tensor field. Metric of the surface depicted as ellipses (*top left*), the parametrized surface (*top right*), HKS on the surface (*bottom right*) and the HKS on U (*bottom right*)

Motivated by these useful properties, the HKS has recently been proposed to visualize symmetric positive definite tensor fields [12]. The basic idea is to consider the HKS as a signature of the metric of the surface. By abstracting completely from the concept of an embedded surface, we can apply the HKS to tensor fields with the characteristics of a Riemannian metric, i.e. symmetric positive definite tensor fields.

The relation between the HKS of a two-dimensional surface M and a positive definite tensor field (i.e. the metric tensor field of the surface) is illustrated in Fig. 1. If g is the metric of the surface M and $f : \mathbb{R}^2 \supset U \mapsto \mathbb{R}^3$ a parametrization of M, i.e. $f(U) = M$, we can compute the pull back of the metric g on U by f, denoted by f^*g. The metric f^*g is a positive definite tensor field on U which is well characterized by the HKS of the surface. We can thereby compute the HKS for a positive definite tensor field defined on $U \subset \mathbb{R}^2$, by interpreting the tensor field as the metric of a surface.

Note that it is not necessary to compute an explicit embedding of the associated surface into some Euclidean space to compute the HKS of a given tensor field. This results in a significant difference for the computation of the HKS. While in case of surfaces the embedding is utilized to compute the HKS, in the case of general tensor fields all computations can be done using the tensor only. To do this efficiently, a realization employing a finite element method is described in [12]. If you are only interested in very short times scales there may be more accurate alternatives for the computation, see e.g. [10].

The concept described above has been successfully applied to positive define tensor fields [12]. For other tensor fields, e.g. stress tensor fields, this method is not directly applicable. In this paper, we propose to interpret such tensor fields as a generator of a time dependent deformation via a positive monotonic mapping, to obtain a field which describes a process close to a diffusion process [5]. This enables us to analyze these fields using the HKS.

A short introduction to the HKS and its application to tensor fields is given in Sect. 2.1. In Sect. 3 we motivate the use of the HKS to indefinite tensor fields and explain its generalization. Experiments and results from applying the method are shown in Sect. 4.

2 Fundamentals

In this section we recall the basic concepts and definitions of the heat kernel and its signature. It follows the original paper [12] closely.

2.1 Heat Kernel Signature

The Heat Kernel Signature (HKS) has been introduced in the field of visualization and computer graphics with the purpose of comparing surfaces. It is derived from the heat equation and assigns each point of the surface a time dependent function, which depends solely on the metric of the surface. The time parameter supports a multiscale comparison. It is used to control the size of the neighborhood of a point on the surface which is taken into account for the HKS. The definition of the HKS is applicable for arbitrary Riemannian manifolds, and thus can be used to visualize more general, positive definite tensor fields. A brief introduction to the HKS is given in this section. For details on the HKS we refer the reader to [11], while a formal treatment of the heat operator and the heat kernel can be found in [9].

Let (M, g) be a compact, oriented Riemannian manifold and Δ the Laplace-Beltrami operator on M which is a equivalent to the usual Laplacian in case of flat spaces. Given an initial heat distribution $h(x)$ on M, the heat distribution $h(t, x)$ at time t is governed by the *heat equation* $(\partial_t - \Delta)h(t, x) = 0$. The *heat kernel* $k(t, x, y)$ is satisfying $(\partial_t - \Delta_x)k(t, x, y) = 0$ with $\lim_{t\to 0} \int k(t, x, y)h(y)\, dy = h(x)$ where Δ_x denotes the Laplacian acting in the x variable. The heat kernel can be computed based on the eigenvalues λ_i and eigenfunctions ϕ_i of Δ by

$$k(t, x, y) = \sum_i e^{-\lambda_i t}\phi_i(x)\phi_i(y) \quad . \tag{1}$$

The heat kernel signature (HKS) is defined in [11] as the function *HKS*

$$HKS(t, x) = k(t, x, x) \ . \tag{2}$$

Since the heat kernel is much more complex than the HKS, one might expect to lose a lot of information when regarding the HKS instead of the heat kernel. But, as shown in [11], the HKS of a surface contains almost all information of the metric of the surface itself and is much more informative than usual scalar quantities like the trace or the determinant. For small values of the time parameter t the HKS is strongly related to the curvature of the manifold. Intuitively, the heat is 'trapped' in regions with positive Gaussian curvature, while there is much 'space to escape' in regions with negative Gaussian curvature.

2.2 HKS for Symmetric Positive Definite Tensor Fields

The HKS introduced above is defined for any compact, oriented Riemannian manifold. Thus the HKS is not restricted to surfaces embedded in $\mathbb{R}^n$. If we have a metric tensor g, i.e. a symmetric positive definite tensor field, defined on a region $U \subset \mathbb{R}^n$, then (U, g) forms a Riemannian manifold. Since there is a Riemannian manifold associated with a positive definite tensor field in this way, we can compute the HKS for any positive definite tensor field. The relation of the HKS for surfaces and tensor fields is based on considering a parametrized surface and the pullback of its metric. This means, given a parametrized surface we can compute the HKS for the surface $f(U)$ or the HKS can be directly computed on U using the metric g even without knowing its embedding. This is equivalent to computing the HKS on the surface $f(U)$ and then pull it back to the parameter space U. This is nicely illustrated in the commuting diagram in Fig. 1. More details are given in the paper by Zobel et al. [12]

An example for the HKS for a symmetric positive definite tensor field is shown in Fig. 2, a diffusion tensor data set of a brain. Instead of using the diffusion tensor T itself we consider the metric $g = T^{-1}$. Large eigenvalues of the diffusion tensor correspond to high diffusivity in direction of the respective eigenvalue, whereas small eigenvalues correspond to low diffusivity. Since a high diffusivity should reflect small distances considering the inverse tensor is a natural way of assigning a metric to a diffusion tensor. For a detailed discussion see [6]. We evaluate the HKS for different time steps. Although the extraction of a single slice might discard valuable information, the structure of the brain becomes obvious by the HKS. The defined metric implies that blue regions (low values) reflect high diffusivity, whereas red regions (high values) reflect low diffusivity. Moreover, the time parameter t allows us to focus on small- as well as large-scale structures.

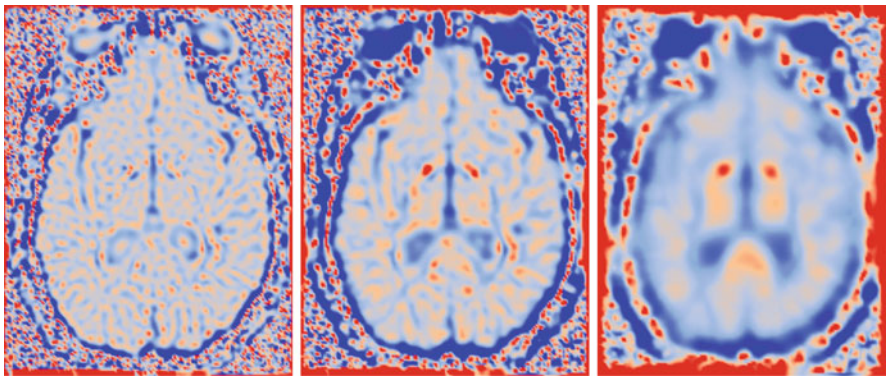

Fig. 2 HKS of a brain data set (Data set courtesy of Gordon Kindlmann at the Scientific Computing and Imaging Institute, University of Utah, and Andrew Alexander, W. M. Keck Laboratory for Functional Brain Imaging and Behavior, University of Wisconsin-Madison.) for different t. The inverse of the diffusion tensor is considered. The colormap ranges from the minimum (*blue*) to the maximum (*red*) of each individual image

2.3 Numerical Realization

The computation of the HKS for symmetric positive definite tensor fields has been described in [12] in detail. The method employs a finite element approach solving a generalized eigenvalue equation of the Laplacian. For the more general application of indefinite tensor fields this approach can be used without any changes. Also the choice of appropriate boundary conditions is discussed in this paper. Usual boundary conditions like Dirichlet or Neumann boundary conditions influence the HKS significantly. Neumann boundary conditions represent a perfectly insulated boundary. Dirichlet boundary conditions cause the HKS to have a fixed value at the boundary. To reduce these boundary artifacts we reflect a part of the field at the boundary such the heat at the boundary can diffuse outwards, see Fig. 3.

3 Using the HKS for Indefinite Stress Tensor Fields

While the relation of the heat diffusion process to other diffusion processes is obvious this is not the case for general indefinite tensors. For some applications however, there are indefinite tensors that can be considered as generator of a deformation process, which is described by a positive definite tensor. One example for such a tensor is the stress tensor, which is a central physical quantity for material modeling in mechanical engineering. In this section we propose an extension of the HKS method introduced by Zobel et al. [12] to a more general setting. The

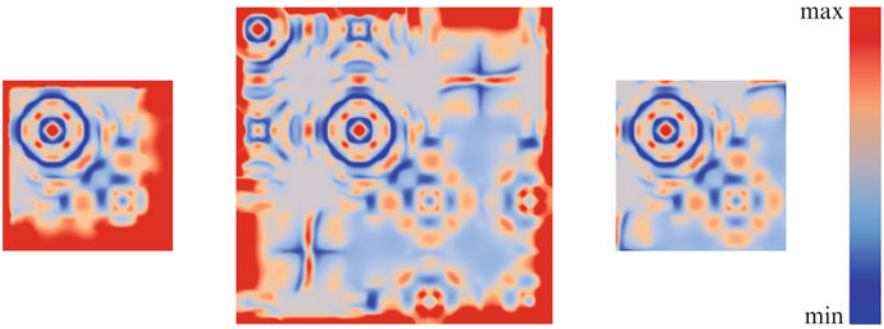

Fig. 3 The result of the two point load data set on the *left* is strongly influenced by the boundary. This effect can be reduced significantly by reflecting a portion of the tensor field on the boundary (*middle*) and cropping the result (*right*)

basic idea is to introduce a natural mapping of stress tensor fields to a positive definite tensor field which serves as input for the HKS computation. To motivate the mapping we will summarize some physical basics related to the stress tensor σ in the following. It should be noted, that this summary depicts a strongly simplified view on the much more complex topic of deformation and stress theory. The intention is mainly to justify the specific choices of mapping functions used for the visualization. We restrict the discussion to two-dimensional tensors to keep it simple. Our current implementation is also restricted to this case. For more details we refer to mechanical engineering textbooks, e.g. [1, 3]. The task of material modeling involves two essential tensor fields: the strain and the stress tensor field.

Considering the deformation of a continuous material, as a response to external forces, the deformation is essentially described by the displacement vector field. The *deformation gradient tensor* F measures all associated changes: stretches (local volume and shape changes) and local orientation changes due to rotations. Neglecting the rotational part, the stretch tensor is then derived from F employing the *polar decomposition*. It is a symmetric, positive definite tensor of second order. The physical quantity generally used for material modeling is *strain*, the relative stretch. In one dimension the uniaxial strain ϵ is defined as logarithm of the relative changes in length L

$$\epsilon = \int \frac{\mathrm{d}L}{L} = \ln \frac{L}{L_0} \quad . \tag{3}$$

Similarly, the multi-axial strain is defined as the logarithm of the rotation free part of the deformation tensor.

The *stress tensor* characterizes the local direction-dependent loads inside of a material. The sign of its eigenvalues are related to compressive respective tensile

forces. Stress σ and strain ϵ tensor are linked through the constitutive relationship, which is close to linear for the large class of linear elastic materials (Hooke's law)

$$\sigma = C\,\epsilon \ ,$$

where C is a tensor of fourth order.

The naive intuition behind the mapping applied for the visualization of the stress tensor corresponds to a 'relaxation' of the material with respect to internal stresses. While the actual deformation process is much more complex, this mapping still gives an idea of a small scale transformation inside the material. In accordance to Eq. (3) the exponential mapping is the natural choice. For small scale changes it can be approximated linearly using the first term of the Taylor expansion. For visualization purposes we consider a larger variety of mappings with similar characteristics. They will be introduced in the following. A similar idea has also be used in [5] for the generation of texture visualizations.

Let T be a two-dimensional symmetric tensor field, $\lambda_1 \leq \lambda_2$ its eigenvalues and U the orthogonal matrix, such that

$$T = U^T \begin{pmatrix} \lambda_1 & \\ & \lambda_2 \end{pmatrix} U \ .$$

We define $\psi(T)$ for any positive, monotonic function $\psi : \mathbb{R} \to \mathbb{R}$ by

$$\psi(T) = U^T \begin{pmatrix} \psi(\lambda_1) & \\ & \psi(\lambda_2) \end{pmatrix} U \ .$$

The tensor $\psi(T)$ is now positive definite while its eigenvector fields remain unchanged. The selection and parametrization of the mapping ψ influences the HKS. Thus this choice has to be made carefully. We use the following mappings

- The exponential mapping $\psi(x) = exp(\alpha x)$, which is the most natural choice for stress tensor fields.
- Linear mapping $\psi(x) = c + \alpha x$, where α and c are constants such that we obtain a positive definite field.
- Arc tangent mapping $\psi(x) = \arctan(\alpha x) + \frac{\pi}{2}$. As for the exponential mapping, the range of this function is limited to $\mathbb{R}^+$. It further enhances changes for small absolute values of stresses while it is asymptotic for stresses with large absolute values.

Experiments using these mappings are shown in Sect. 4.

4 Results

In this section, we discuss some results of first experiments with indefinite stress tensor fields. We investigate the sensitivity of the HKS with respect to the three different mapping functions described in the previous section and the involved parameters. Therefore we consider two data sets which are both results from numerical finite element simulations of material stressing. Both data sets are originally three-dimensional, of which we have extracted two-dimensional slices. The first data set simulates two forces acting on a solid block, one pulling, one pushing the 'two point load'. This is a simulation with a very low resolution exhibiting some discretization artifacts, leading to a small scale structure. This data set is well-studied and therefore appropriate to evaluate our method. Throughout this section we use the colormap shown in Fig. 3, which ranges from the minimum to the maximum for the respective data set and setting.

We start with the exponential mapping, which is the most natural choice with respect to the physical interpretation. More precisely, we consider the tensor fields $\exp(T)$ (Fig. 4 first row) and $\exp(0.01T)$ (Fig. 4 second row), i.e. we use two different scalings of the original field. We can observe that the different scaling has hardly any influence on the result using this color map (from min blue to max red). Further, the HKS is evaluated for different time steps t. We see that for small time scales all details of discretization artifacts of the simulation are visible. Moving to larger times these details vanish and only the major features, the pushing and the pulling force remain.

In Fig. 5 the arc tangent mapping is applied to the tensor field. This mapping is symmetric with respect to positive and negative eigenvalues. It especially emphasizes changes for eigenvalues with small absolute value while the mapping

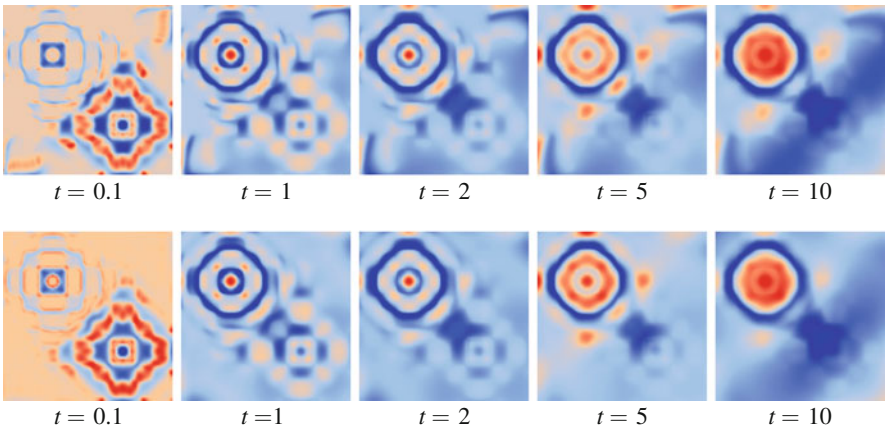

Fig. 4 HKS of a two point load data set (Data set courtesy of Boris Jeremić, University of California Davis.) using the exponential mapping. *First row* $\exp(T)$, *second row* $\exp(0.01T)$

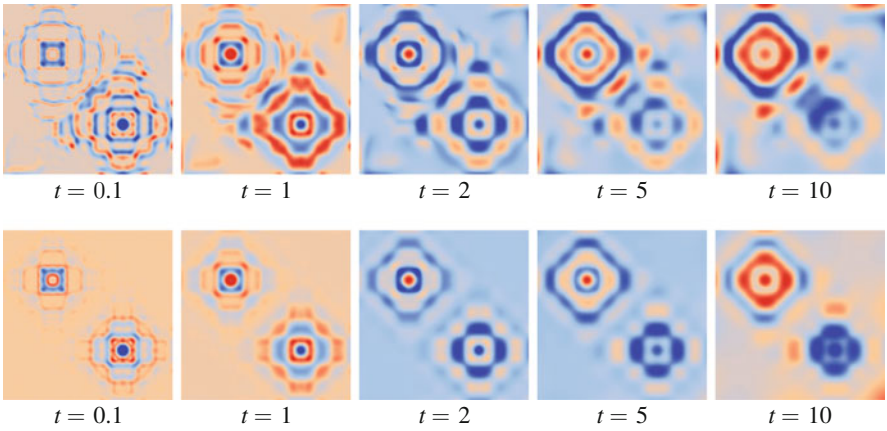

Fig. 5 HKS of a two point load data set mapped by arctan, scaled with $\alpha = 0.1$ for the *first row* and $\alpha = 0.001$ *second row*

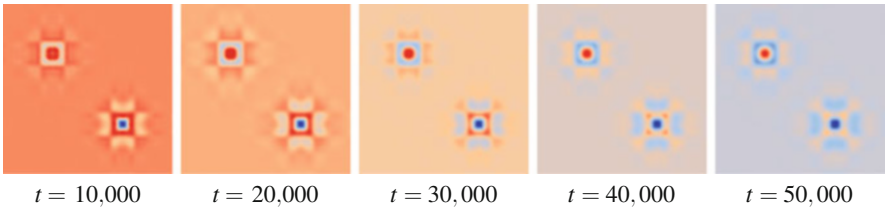

Fig. 6 HKS of a two point load data set using the linear mapping

is asymptotic for eigenvalues with large absolute value. In our example the tensor field is scaled with 0.1 and 0.001 in the first and second row, respectively, and shifted by $\frac{\pi}{2}$ to obtain a positive definite field, i.e. we consider $\arctan(0.1T) + \frac{\pi}{2}$ and $\arctan(0.001T) + \frac{\pi}{2}$. Using the arc tangent mapping, the scaling has more impact than for the exponential mapping. While the scaling of 0.1 also emphasizes regions with small eigenvalues of the tensor T, the scaling of 0.001 focuses on regions with more extremal eigenvalues, i.e. the points where the load is applied.

The simplest approach to obtain a positive definite tensor field is to shift the eigenvalues of T by a constant, such that the smallest eigenvalues occurring in the field are just above zero. Such a linear mapping is used in Fig. 6. Since the eigenvalues of our data set range from about $-27{,}500$ to $27{,}500$, we add $27{,}500$ to all eigenvalues. Therefore the area represented by the resulting metric is much larger than for the preceding mappings. As a consequence much larger time values have to be considered. However, the different time steps still show a very similar behavior. Shifting the eigenvalues by a constant causes the metric to represent a larger area at each point, thus the curvature decreases. Consequently there seem to arise some peaks of the curvature at points where the eigenvalues are close to the minimum, which dominate the behavior of the HKS for all time values. Thus, the

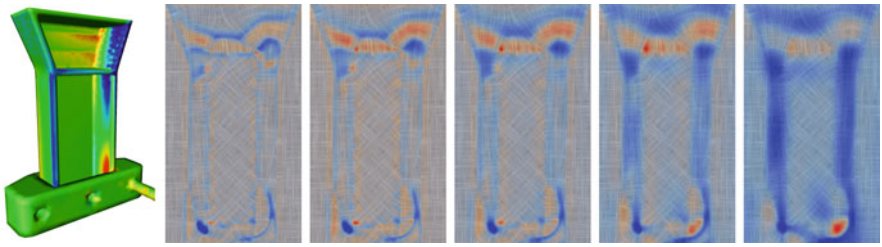

Fig. 7 HKS of a two point load data set with exponential mapping, scaled with $\alpha = 100$. The principal stress directions of the data set are given as context information in the background texture. Data courtesy Markus Stommel, TU Dortmund, Germany

linear mapping is maybe not the proper choice to obtain a positive definite tensor field, at least if there are strong negative peaks in the smallest eigenvalue field.

A second example represents the simulation of a mechanical work piece, see Fig. 7. It consists of a boundary structure filled with a fictitious material with a very low Young's modulus. Within the interior of the filled region the stresses are almost constant. The small scale HKS clearly emphasizes the discontinuities in the material selection. For larger scales it can be seen which parts of the material are more responsive to the applied forces.

5 Conclusion and Future Work

By applying a respective mapping to indefinite tensor fields it is possible to compute the heat kernel signature for such fields. This provides a new visualization method for stress tensors which differs strongly from common visualization methods. Due to its sensitivity with respect to the derivative of the tensor field it conveys additional information which is not visible in direct visualization. A special strength of the method is its inherent level of detail property. Thus, it is possible to emphasize smaller or larger structures. In contrast to basic Gaussian smoothing the scaling is directly driven by the tensor data itself. On the other side the interpretation of the results is not as easy and requires some effort. There are still many open questions in this respect. For the future we plan on further investigating the significance of the HKS for further applications. It might be of interest to compare the scaling properties to ideas of anisotropic diffusion.

From a theoretical point of view the method can be easily generalized to 3D tensor fields. With the exception of the formulas indicating the relation to Gaussian curvature, all statements are also valid in higher dimensions. The main obstacle is that the computation of the eigenvalues and eigenfunctions of the Laplacian is non-trivial. The computation of the first 500 eigenvalues for a data set with 256^2 points

already takes a few minutes, thus the computation time for a data set with 256^3 points is going to be infeasible using standard approaches.

References

1. Brannon, R.M.: Functional and structured tensor analysis for engineers. UNM Book Draft (2003). http://www.mech.utah.edu/~brannon/
2. Bronstein, M., Kokkinos, I.: Scale-invariant heat kernel signatures for non-rigid shape recognition. In: 2010 IEEE Conference on Computer Vision and Pattern Recognition (CVPR), pp. 1704–1711 (2010)
3. Danielson, D.A.: Vectors and Tensors in Engineering and Physics, 2nd edn. Department of Mathematics, Naval Postgraduate School, Monterey, CA. Addison-Wesley, Reading, MA (1997) [Diss]
4. Dey, T., Li, K., Luo, C., Ranjan, P., Safa, I., Wang, Y.: Persistent heat signature for pose-oblivious matching of incomplete models. In: Computer Graphics Forum, vol. 29, pp. 1545–1554 (Wiley Online Library, 2010)
5. Hotz, I., Feng, L., Hagen, H., Hamann, B., Jeremic, B., Joy, K.I.: Physically based methods for tensor field visualization. In: VIS '04: Proceedings of IEEE Visualization 2004, pp. 123–130. IEEE Computer Society Press, Los Alamitos (2004)
6. O'Donnell, L., Haker, S., Westin, C.F.: New approaches to estimation of white matter connectivity in diffusion tensor mri: elliptic pdes and geodesics in a tensor-warped space. In: Medical Image Computing and Computer-Assisted Intervention MICCAI 2002, pp. 459–466. Springer, Berlin (2002)
7. Ovsjanikov, M., Bronstein, A., Bronstein, M., Guibas, L.: Shape Google: a computer vision approach to isometry invariant shape retrieval. In: 2009 IEEE 12th International Conference on Computer Vision Workshops (ICCV Workshops), pp. 320–327 (2009)
8. Raviv, D., Bronstein, M., Bronstein, A., Kimmel, R.: Volumetric heat kernel signatures. In: Proceedings of the ACM Workshop on 3D Object Retrieval, pp. 39–44 (2010)
9. Rosenberg, S.: The Laplacian on a Riemannian Manifold: An Introduction to Analysis on Manifolds. Cambridge University Press, Cambridge (1997)
10. Spira, A., Sochen, N., Kimmel, R.: A short time beltrami kernel for smoothing images and manifolds. IEEE Trans. Image Process. **16**(6), 1628–1636 (2007)
11. Sun, J., Ovsjanikov, M., Guibas, L.: A concise and provably informative multi-scale signature based on heat diffusion. In: Proceedings of Eurographics Symposium on Geometry Processing (SGP) (2009)
12. Zobel, V., Reininghaus, J., Hotz, I.: Visualization of two-dimensional symmetric positive definite tensor fields using the heat kernel signature. In: Topological Methods in Data Analysis and Visualization III, pp. 249–262. Springer, Berlin (2014)